Kinetics of Switchable Proton Escape from a Proton-Wire within Green Fluorescence Protein

Noam Agmon*

Department of Physical Chemistry and the Fritz Haber Research Center, The Hebrew University, Jerusalem 91904, Israel

Received: February 19, 2007; In Final Form: April 29, 2007

The emission from the acidic form of the green fluorescence protein (GFP) changes with increasing time and temperature from $t^{-1/2}$ to $t^{-3/2}$ asymptotics. It is shown that a model of proton diffusion along a one-dimensional hydrogen-bond network within the protein, with a switch (Thr203) allowing for proton escape, explains the data quantitatively. From a comparison of the model with experiment, we obtain the rate parameters for proton dissociation from the chromophore (showing an *inverse* temperature effect), the ratio of the proton association constant squared to its diffusion constant (exhibiting no temperature effect), and the time constant for switch opening (with a significant Arrhenius dependence). Thus, proton dissociation has a small negative activation energy (assigned to a complex of the anionic chromophore with H_3O^+), whereas the switch has a large positive activation energy (assigned to Thr203 side-chain rotation). Proton migration is possibly the outcome of the concerted motion of several protons within GFP.

1. Introduction

Protons participate in numerous enzymatic reactions, are pumped across the cell membrane by bioenergetic proteins during energy transduction process,[1] utilized in ATP synthesis, and allow communications between active sites of an enzyme.[2] The shuttling of protons through proteins most likely occurs only along well-defined hydrogen-bond (HB) networks, composed predominantly of internal water molecules and oxygen atoms on protein side chains (or backbone carbonyls). The interoxygen distance must be below about 3 Å to allow efficient proton hopping between adjacent moieties. Yet, it is rare to find these required "stepping stones" in the X-ray structure. Some of the water molecules are usually labile, entering transiently from solution to complete the wire along which the proton then migrates. The structurally robust green fluorescence protein (GFP) maintains well-defined proton wires allowing an experimental−theoretical investigation of proton migration along a proton-wire on the picosecond−nanosecond time scale, with possible gated escape to the protein surface.

GFP is a prominent biological fluorescence marker.[3] Upon illumination, its chromophore undergoes a reaction of excited-state (ES) proton transfer (ESPT[4]), whence its anion is responsible for the bright green fluorescence.[5,6] X-ray diffraction shows[7,8] that the chromophore is housed within a rigid barrel-like structure of 11 β-sheets, which cannot easily exchange water with solution. The conventional models[8,9] for the photodissociated proton suggest a three-step migration from Tyr66 (which is part of the chromophore), via a water molecule and Ser205, to the (presumably anionic) carboxylate of the buried Glu222 residue (Figure 1). Proton arrival to Glu222 was corroborated by time-resolved IR of GFP in D_2O, where the 1711 cm^{-1} absorption[10] of the carbonyl of protonated Glu222 appears to reach a maximum (around 300 ps in H_2O).[10−12] Recent quantum chemistry calculations,[13,14] for a gas-phase cluster containing the chromophore and the HB chain up to Glu222, suggest that the first step in the relay is the Ser205 → Glu222 transfer, whereas the Tyr66 → water step occurs last. Unfortunately, there is a large quantitative discrepancy between the calculations,[14] and the barrier for the first suggested step (42 kJ/mol)[13] is too large to allow proton transfer within a few picoseconds.[5,6]

The proton-wire is in fact much more extended than it is usually considered, continuing from Glu222 up to Glu5 on the protein's surface.[15] A portion of this path is shown in Figure 1. In addition, the rotation of Thr203 creates an alternate short pathway leading, via the backbone carbonyl of His148, to the protein surface (Figure 1).[15] Analogous proton wires were recently found in asFP595, an optically switchable protein related to GFP (see Figure 4 in ref 16).

Evidence that proton migration within wild-type (wt) GFP is not a simple 1−3 step transfer to Glu222 comes from the time-resolved fluorescence measurements of Huppert and coworkers.[17−19] When the room-temperature fluorescence from the excited protonated form of the chromophore (R*OH) was followed to $t > 10$ ns, a markedly nonexponential decay was observed.[17] When corrected for the ES decay (rate constant k_f) by the factor $\exp(k_f t)$, a long-time $t^{-3/2}$ was revealed. Superficially, this looks like ESPT in solution, which routinely shows such a tail due to reversible adiabatic geminate recombination of the proton, diffusing in three-dimensional (3D) space, with the excited anion.[4,20] This was therefore interpreted as 3D diffusion within the GFP barrel.[17,18] However, the X-ray structure[7,8] has only a few water molecules within the protein, not enough to support 3D diffusion.[15] An alternative possibility, of proton exit to solution with reversible entry, was ruled out because the kinetics showed no effect of varying proton scavenger concentrations in solution.[17]

A recent study of the temperature dependence (T) of the transient emission showed an even more intricate behavior.[19] Below 230 K, the lifetime-corrected fluorescence signal developed a long-time $t^{-1/2}$ tail, much slower than the room-temperature $t^{-3/2}$ asymptotic behavior. It is in fact so prominent

* Corresponding author. Telephone: 972-2-6585687. Fax: 972-2-6513742. E-mail: agmon@fh.huji.ac.il.

10.1021/jp071403p CCC: $37.00
Published on Web 06/15/2007

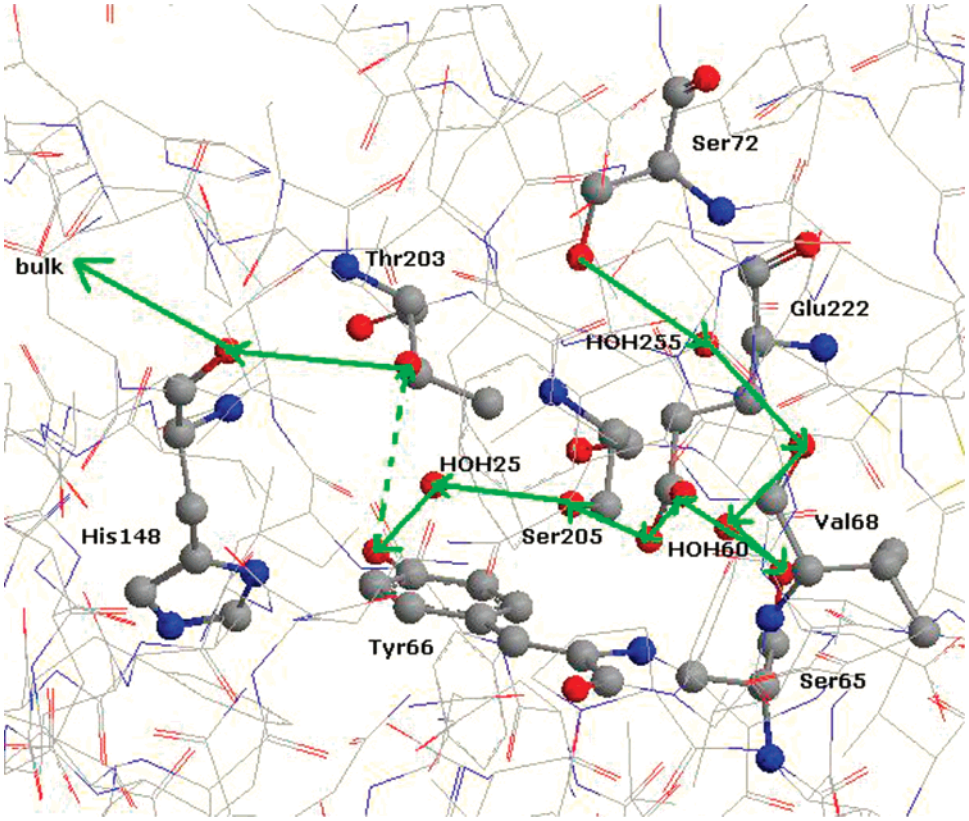

Figure 1. Two proton wires (green) leading to the chromophore inside the wt-GFT. This figure was prepared by Ai Shinobu from PDB file 1GFL[7] using Chem3D version 9.

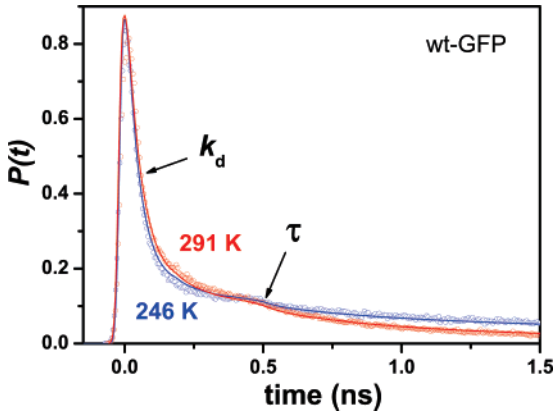

Figure 2. Time-resolved fluorescence from wt-GFP in an aqueous solution containing 30% glycerol at two temperatures, corrected for fluorescence decay (radiative and nonradiative) with a rate constant $k_f = 0.35\ ns^{-1}$. Data points from Figure 5 of ref 19 are courtesy of Dan Huppert. Lines are numerical solutions of the 1D switchable-diffusion model, eqs 3, 11, and 15, with the parameters of Table 1. The calculation was normalized and convoluted with an experimentally measured IRF (fwhm of 40 ps). The bump around 400 ps is due to a small secondary peak in the IRF. The regions in the kinetics controlled by proton dissociation (k_d) and switch opening (τ) are indicated. The effect that the dissociation rate and long-time tail are enhanced at the lower temperature is visible.

that it can readily be seen on a linear scale (Figure 2). As T increases above 230 K, the asymptotic behavior gradually switches to a $t^{-3/2}$ decay;[19] see Figure 3. In addition, the dissociation rate coefficient, k_d, appeared to *decrease* with increasing T in this regime.[19]

The $t^{-1/2}$ tail was tentatively attributed to proton migration along the one-dimensional (1D) proton wire, with occasional reversible recombination with the excited anion of Tyr66.[19] For the observation of diffusive behavior, the wire must be much longer than the three steps separating Tyr66 and Glu222; thus, its continuation toward Glu5 (Figure 1) must be accessed.[15] Yet, the end of the wire is not reached even by 10 ns; otherwise, the fluorescence tail would switch to exponential. It is not self-evident that proton motion along an HB wire should look diffusive, this requires relatively uniform barriers between the proton translocating moieties. If one was to extrapolate from the gas-phase quantum-mechanical energy profiles calculated for the Tyr66−Glu222 proton-wire segment in GFP,[13,14] they might seem too rugged to support diffusion. Yet, one should reserve judgment until full coupling to the GFP protein modes is included in the calculation. Several algorithms for achieving this goal are now available.[21,22]

Consequently, to make a convincing case for the diffusion model one needs to resolve the $t^{-3/2}$ conundrum, explaining how this change in slope comes about. If $t^{-3/2}$ is not a sign for diffusion in 3D, what then is its origin? Here, we show how it arises from an added kinetic step to the 1D model.

The resolution is based on a recent theoretical work which solved analytically the problem of 1D ES diffusion-influenced reversible geminate recombination with an added quenching reaction:[23]

$$R^*OH \underset{k_a}{\overset{k_d}{\rightleftharpoons}} R^*O^- + H^+ \xrightarrow{k_q} RO^- + H^+ \qquad (1a)$$

The excited chromophore, R*OH, dissociates with a rate constant k_d to produce a geminate pair of an excited anion, R*O$^-$, and proton at close proximity ("contact distance"). Both species here have the same ES lifetime, $1/k_f$ (as previously assumed for GFP),[19] though k_f for R*OH can be inferred only indirectly due to the competing ESPT reactions.[4] (The equations can be solved even for differing lifetimes in either 1D or 3D.[23,24]) The geminate pair can separate by diffusion (mutual diffusion

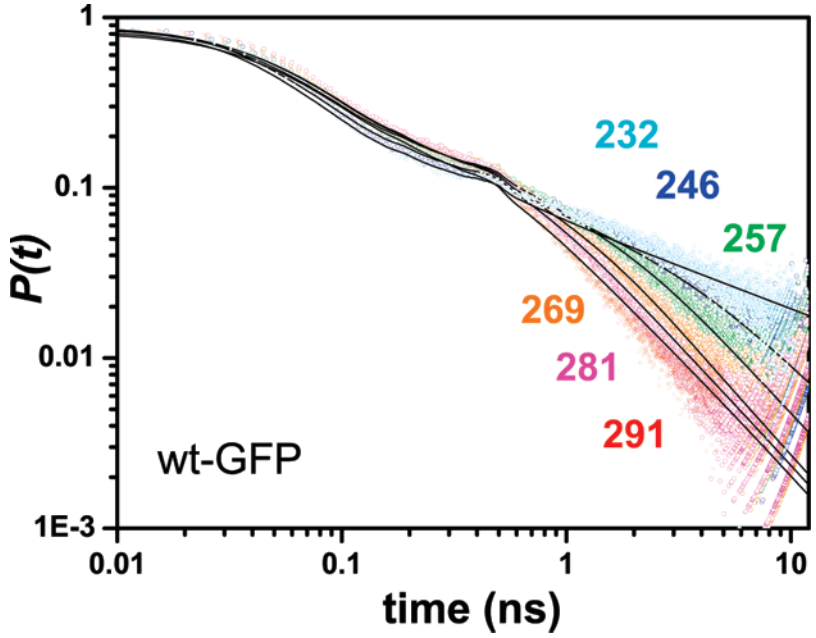

Figure 3. Temperature dependence of time-resolved fluorescence from wt-GFP displayed on a log−log plot for the six indicated temperatures (in kelvin). See Figure 2 for other details.

constant D), recombine adiabatically to reform the excited chromophore (rate constant k_a), or the proton quenches the chromophore to its ground state (rate constant k_q). The ES kinetics were solved also for an interaction potential,[25,26] but the present exposition is limited to the interaction-free case.

A central result of ref 23 is that the asymptotic decay of the R*OH population in 1D changes from $t^{-1/2}$ (for $k_q = 0$) to $t^{-3/2}$ (for $k_q \neq 0$). Therefore, a $t^{-3/2}$ tail does not necessarily imply diffusion in 3D, as previously assumed for the GFP data.[17] It can arise from the opening of the threonine switch that allows irreversible proton escape. Here, we present a quantitative model for explaining this behavior.

The escape problem is isomorphic to the quenching problem, because both processes eliminate the R*OH emitter:

$$\mathrm{R^*OH} \underset{k_a}{\overset{k_d}{\rightleftharpoons}} \mathrm{R^*O^-} + \mathrm{H^+}\,(\mathrm{wire}) \xrightarrow{k_{out}(t)} \mathrm{R^*O^-} + \mathrm{H^+}\,(\mathrm{out}) \quad (1b)$$

However, this requires a time-dependent $k_{out}(t)$, instead of a fixed k_q, for depicting the kinetics of the switch. This may be solved analytically (see section 2) if the opening occurs instantaneously at some time $\tau > 0$. The problem for more complex $k_{out}(t)$ is solved numerically, using a Windows application for the spherically symmetric diffusion problem (SSDP).[27] The results (see section 3) suggest that the R*OH fluorescence from GFP is tracking, in real time, proton dissociation, its diffusion along an internal proton-wire, and its ultimate irreversible escape via a switchable exit route (see section 4).

2. Theory

We consider now a theoretical model for the kinetics in eq 1b occurring along a 1D proton wire. Let us first summarize the relevant results[23] for particle diffusion along a semi-infinite line (diffusion constant D), with reversible recombination plus irreversible escape occurring from a point nearest to the recombined state. Subsequently, we consider the effect of adding a switch (with an opening time-constant τ) for modulating the escape probability. The model is depicted schematically in Figure 4.

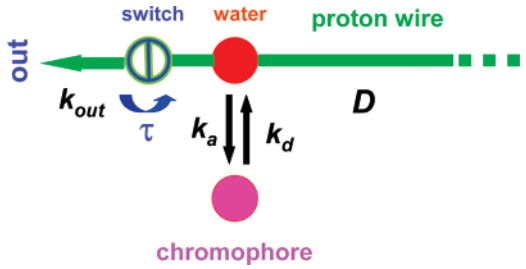

Figure 4. Schematic depiction of the switchable diffusion model solved in the present work.

In application to experiment, the transient fluorescence data are first multiplied by $\exp(k_f t)$, where k_f is obtained from the long time decay of the R*O$^-$.[19] The diffusing particle is the dissociated proton, the line is the proton-wire, the bound state (designated by an asterisk) is the ES chromophore. When the switch is open, the proton may also exit irreversibly from the $x = 0$ end of the proton-wire, which is the water molecule adjacent to Tyr66. Ignoring any potential of interaction for the particle, the model involves a 1D free-diffusion equation with appropriate boundary conditions.

2.1. Fixed Escape Rate Constant. Denote by $p(x,t|x_0)$ the probability of observing the diffusing particle (the proton) at location x by time t, given that it was initially at x_0. Its time evolution obeys:[23]

$$\frac{\partial p(x,t|x_0)}{\partial t} = D\frac{\partial^2}{\partial x^2}p(x,t|x_0) + [k_d p(*,t|x_0) - (k_a + k_q)p(x,t|x_0)]\delta(x) \quad (2)$$

This is a 1D diffusion model for the kinetic scheme in eq 1a. The delta-function limits the reaction to occur at $x = 0$, the closest point to the bound state, $*$ (the protonated ES chromophore, R*OH). From $*$, dissociation to $x = 0$ occurs with a rate constant k_d. From $x = 0$, two competing reactions occur: association to reproduce $*$ with a rate-constant k_a and escape with a rate-constant k_q.

The above equation is coupled to an ordinary differential equation for the "binding probability", $p(*,t|x_0)$, which is the probability that the particle is bound given that it was initially unbound and at $x = x_0$. Its time evolution is depicted by the rate equation

$$dp(*,t|x_0)/dt = k_a p(0,t|x_0) - k_d p(*,t|x_0) \quad (3)$$

Note that k_q does not appear here, since escape occurs from $x = 0$ into a state different from $*$. A related model, where escape occurs from the bound-state can also be formulated and it leads to qualitatively similar results. However, the HB formed between Tyr66 and Thr203 may change k_d and k_a, so it seems preferable to consider exit as occurring in a single step from the adjacent water molecule.

One is eventually interested in the solution for an initially bound particle, $p(x,t|*)$, obtainable via the detailed balance condition

$$k_a p(x,t|*) = k_d p(*,t|x) \quad (4)$$

From it, one calculates $P(t) \equiv p(*,t|*)$, which corresponds to the experimentally measured signal of the R*OH, after multiplication by $\exp(k_f t)$.

The above equations are solved[23] by the Laplace transform method. After some manipulations, one obtains an expression with a quadratic polynomial in the denominator. The three roots of this polynomial, $-\alpha$, $-\beta$, and $-\gamma$ are related to the three rate constants by the following:

$$\alpha + \beta + \gamma = (k_a + k_q)/D \quad (5a)$$

$$\alpha\beta + \beta\gamma + \gamma\alpha = k_d/D \quad (5b)$$

$$\alpha\beta\gamma = k_d k_q/D^2 \quad (5c)$$

The three roots allow separation of the above-mentioned expression into three terms, which can then be inverted. The binding probability becomes[23]

$$P(t) = \frac{\alpha(\beta+\gamma)}{(\gamma-\alpha)(\alpha-\beta)}\Omega(\alpha\sqrt{Dt}) + \frac{\beta(\gamma+\alpha)}{(\alpha-\beta)(\beta-\gamma)}\Omega(\beta\sqrt{Dt}) + \frac{\gamma(\alpha+\beta)}{(\beta-\gamma)(\gamma-\alpha)}\Omega(\gamma\sqrt{Dt}) \quad (6)$$

Here, $\Omega(z)$ is the ubiquitous function

$$\Omega(z) = \exp(z^2)\,\mathrm{erfc}(z) \quad (7)$$

where $\mathrm{erfc}(z)$ is the complementary error function of a possibly complex variable z.[28]

In the special case that $k_q = 0$ (designated below by a subscript 0), we can set $\gamma = 0$ in eq 5c, obtaining $\alpha + \beta = k_a/D$ and $\alpha\beta = k_d/D$. In this limit, eq 6 reduces to

$$P_0(t) = \frac{1}{\beta-\alpha}[\beta\Omega(\alpha\sqrt{Dt}) - \alpha\Omega(\beta\sqrt{Dt})] \quad (8)$$

as previously found.[29]

The long-time asymptotic behavior of $P(t)$ can be obtained from that of the complementary error function.[28] Two different behaviors are found.[23] When $k_q > 0$, the asymptotic behavior is

$$P(t) \sim \frac{k_a}{{k_d k_q}^2}\sqrt{\frac{D}{\pi t^3}} \quad (9a)$$

This extends to any initial location, x_0, of the particle

$$p(*,t|x_0) \sim \left(1 + \frac{k_q x_0}{D}\right)P(t) \quad (9b)$$

However, if $k_q = 0$, a different behavior is obtained

$$P_0(t) \sim \frac{k_a}{k_d}\sqrt{\frac{1}{\pi D t}} \quad (10)$$

Thus, the vanishing of k_q induces a transition from a $t^{-3/2}$ to a $t^{-1/2}$ behavior. Note also that D has opposite effects on the magnitude of the long-time tail of $P(t)$ for the two cases. When $k_q > 0$, faster migration on the wire enhances the tail, since it competes with the escape process. When $k_q = 0$, migration on the wire reduces the probability of recombination.

2.2. Time-Dependent Escape Rate Constant. The theory can now be extended to a switch that opens with a time dependence $k_{out}(t)$, eq 1b, by rewriting eq 2 as follows:

$$\frac{\partial p(x,t|x_0)}{\partial t} = D\frac{\partial^2}{\partial x^2}p(x,t|x_0) + \{k_d p(*,t|x_0) - [k_a + k_{out}(t)]p(x,t|x_0)\}\delta(x) \quad (11)$$

This is coupled to eq 3, which remains without change. In the simple case, that the switch opens abruptly at some time $\tau > 0$, we have

$$k_{out}(t) = k_q H(t-\tau) \quad (12)$$

where $H(y)$ is the Heaviside function: $H(y) = 1$ for $y > 0$ and $H(y) = 0$ otherwise. For $t < \tau$, the kinetics starts approaching the $t^{-1/2}$ asymptotics of eq 10. When the switch opens, at $t = \tau$, the distribution density is $p_0(x,\tau|*)$ and this $k_q = 0$ solution can be found analytically.[23,29] For $t > \tau$, there is an added escape route which enhances the R*OH decay. The kinetics now approach a new asymptotics, obtained by averaging eqs 9 over $p_0(x,\tau|*)$:

$$P(t) \sim \left(1 + \frac{k_q \bar{x}_0(\tau)}{D}\right)\frac{k_a}{{k_d k_q}^2}\sqrt{\frac{D}{\pi t^3}} \quad (13)$$

where $\bar{x}_0(\tau) \equiv \int_0^\infty x p_0(x,\tau|*)\,dx$. (Here, we have assumed that $t - \tau \to t$ for large t values.) Thus, the switch-opening kinetics adds a second term to eq 9a, albeit with the same $t^{-3/2}$ behavior. This demonstrates that a $t^{-1/2} \to t^{-3/2}$ transition will eventually occur regardless of when the switch opens.

A more physical situation is realized for opening via first-order reaction kinetics (rather than instantaneously)

$$\text{close} \xrightarrow{1/\tau} \text{open} \quad (14)$$

It is likely irreversible due to the rather strong HB formed between the rotated Thr203 and the anion of Tyr66. The exit rate constant can then be written as

$$k_{out}(t) = k_q[1 - \exp(-t/\tau)] \quad (15)$$

This is a product of the opening probability by the proton exit rate constant, k_q. Equation 11 with this time-dependent $k_{out}(t)$ cannot be solved analytically, but it may readily be solved numerically.[27] In addition to τ, which governs the switch kinetics, the solution depends on three parameters characteristic of the proton kinetics: k_d, $k_a/\sqrt{D}$, and $k_q/\sqrt{D}$. As discussed in detail elsewhere,[30] from fitting time-dependent observables, it

TABLE 1: Temperature Dependence of the Model Parameters for the Data in Figures 2 and 3[a]

T (K)	τ (ns)	k_d (ns^{-1})	k_a/k_q
291	0.45	42	3.2
281	0.7	42	3.2
269	1.3	42	3.2
257	2.0	51	4.4
246	3.5	61	7.3
232	∞	65	∞

[a] Global parameters: $k_f = 0.35$ ns^{-1}; $k_a^2/D = 6.4$ ns^{-1}.

is not possible to determine distance-dependent parameters. Therefore, one cannot obtain k_a, k_q, and D individually, only their spatially independent ratios.

3. Results

Time-resolved emission from wt-GFP (in 30% aqueous glycerol solutions) at various temperatures was reported by Leiderman et al.[19] (see their Figure 5). These time-correlated single-photon counting (TCSPC) data span a time scale from 40 ps, the instrument response function (IRF) width, to over 10 ns. Yet, careful convolution with the IRF allows the resolution of processes as fast as 20 ps. The intensity here varies by 3 orders of magnitude *after* correcting for the excited-state decay by multiplying the data by $\exp(k_f t)$. Hence, although the TCSPC method lacks in time resolution as compared with upconversion,[5] pump−probe,[31] or transient IR[10−12] techniques, it has an unprecedented dynamic range and signal-to-noise ratio. Moreover, its signal arises *only* from the ES dynamics (whereas transient absorption contains contributions also from the ground state). The study in ref 19 is presently the only systematic temperature study of GFP kinetics, and this will allow us to obtain the activation energies for the processes involved.

The data between 110 and 220 K exhibit a long-time decay which follows a $t^{-1/2}$ power law,[19] but from 230 K to room temperature, there is a switchover to $t^{-3/2}$ asymptotics, which occurs at shorter times with higher temperatures. The data above 230 K, shown as points in Figures 2 and 3, will be analyzed below.

Using the 1D diffusion model of section 2, we solve eq 11 with the escape rate coefficient of eq 15 and coupling to eq 3. The SSDP program[27] (version 2.66) is utilized to obtain the numerical solution, convolute with the IRF, and compare with the data, iterating (manually) until a suitable fit is obtained. The total length of the diffusion interval, $[0,x_{max}]$, is chosen so that 10^{-10} of the population accumulates at an absorbing boundary imposed at x_{max}. Under these conditions, this interval is practically infinite (and the boundary condition at x_{max} is immaterial). The R*OH state is implemented with the reversible boundary condition of SSDP (at $x = 0$). The added irreversible sink there, $k_{out}(t)$, is implemented as a square "delta function" of width $x_{max}/100$ at the origin. The value of $k_{out}(t)$ is updated every time-step using the "updating" option of SSDP. (Note that the "double boundary" option is not utilized due to a bug when implemented with time-dependent functions.)

The best-fit parameters are collected in Table 1. Global parameters, which do not depend on T, are k_f and k_a^2/D. The remaining three parameters were adjusted at each temperature: k_d, τ, and k_q/k_a. The first two are discussed in detail below.

Figure 5 shows log (k_d) as a function of $1/T$ down to 232 K. When the data point at 291 K is eliminated, the behavior roughly follows an Arrhenius equation

$$k_d = A \exp(-E_A/RT) \qquad (16)$$

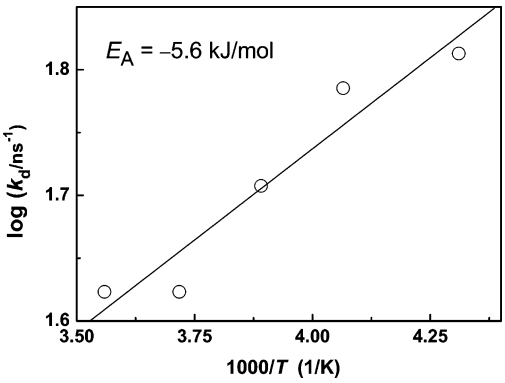

Figure 5. Arrhenius plot for the proton dissociation rate constant from wt-GFP above 230 K (k_d, Table 1) showing a negative activation energy of −5.6 kJ/mol.

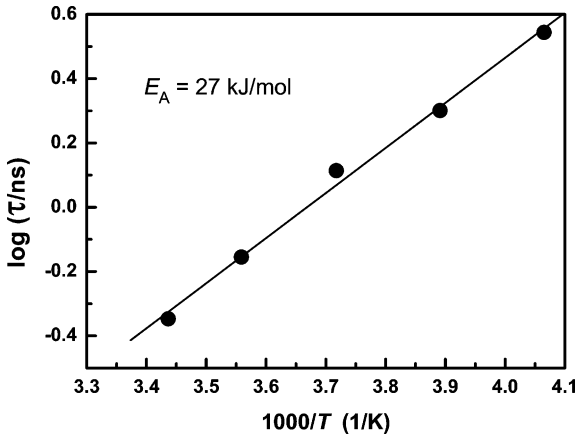

Figure 6. Arrhenius plot for the switch opening times (τ, Table 1) as a function of inverse temperature. The slope yields an activation enthalpy of 27 kJ/mol.

R being the gas constant. The figure shows that k_d *increases* with decreasing T, with a *negative* activation energy of −5.6 kJ/mol. Admittedly, the values of k_d may have a large error, since the dissociation times are within the IRF of the TCSPC method. It may represent an effective rate constant for two-step kinetics observed in measurements with better time resolution.[5,6] Yet, the inverse temperature effect, deduced already in ref 19, is corroborated here by a quantitative fit over the whole time range.

Figure 6 shows an Arrhenius plot for τ. Now, there is a "normal" temperature effect with a (relatively) large and positive activation energy of 27 kJ/mol. In our model, this quantity represents the barrier for the threonine side-chain rotation (including a small possible contribution from hydrogen-bonding of its hydroxyl group prior to rotation).

It is interesting to check how uniquely the kinetic data determine the kinetic model presented herein. Clearly, one cannot check all conceivable kinetic models, but the following example may convince some that a model which fits the data over such a large time/temperature range is sensitive to the details of the mechanism. Suppose the escape process originates at some point $x > 0$ along the proton wire, rather than at the origin. Figure 7 shows a calculation using the parameters of the 281 K data, except that the delta-function is moved to a distance $4x_{max}/100$ from the origin (blue line). The delay-time τ becomes irrelevant now, because a larger delay is already introduced by the diffusion time to this distance. Therefore, the decay follows the $t^{-1/2}$ law for a longer period of time, and then, it drops more abruptly to the *same* asymptotic behavior as before. This behavior does not have the correct shape to fit

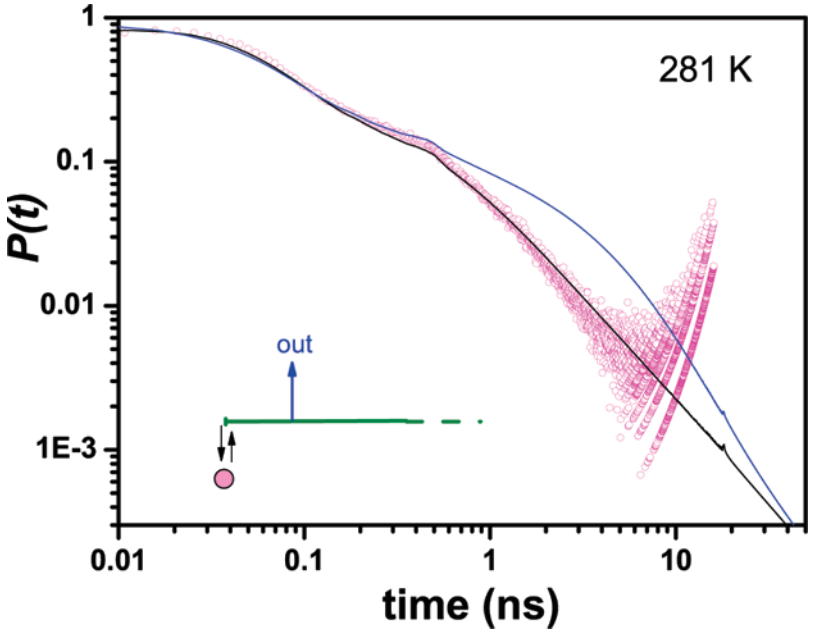

Figure 7. Comparison of an alternative model, with the exit wire branching down the main wire at a distance 4 times the width of the delta-function sink (inset). Calculations, performed with the parameters of the 281 K data in Table 1, are depicted for the original and alternative models by the black and blue lines, respectively.

the data, even if some of the other parameters are readjusted. This seems to rule out the possibility that the proton is trapped at some distant site that connects to the wire past Glu222, rather than exiting directly from the vicinity of the dissociation site.

4. Discussion

While GFP is a protein with widespread biotechnological applications, less attention was paid to the mechanism by which it shuttles its proton. GFP is a unique protein in terms of its rigid barrel structure and, particularly, in terms of its chromophore which is synthesized *in situ* from three consecutive amino-acid side chains. Commensurate with this rigid structure, well-formed HB networks are found within the protein (Figure 1), that may conduct the proton to/from the chromophore.[15,19] In addition, there is a rotatable threonine side chain that can connect to the active site and possibly allow the proton to escape to the protein exterior. The present work establishes, via a simple 1D diffusion model, the mode of operation of these conduction elements.

4.1. Proton Dissociation. Although the TCSPC measurements analyzed herein are of limited temporal resolution, their large dynamic range allow for a more reliable determination of the rate parameters, including k_d, which governs the initial decay of the R*OH fluorescence signal by ESPT. These measurements also provide a first systematic temperature study, revealing a rather unusual (inverse) temperature effect on k_d above 230 K (Figure 5). This contrasts with ESPT in solution,[32] which always exhibits a positive activation energy, E_A.

A negative E_A is usually taken as evidence that the measured rate constant is an effective one, for a microscopically multistage reaction.[33,34] $E_A < 0$ can arise in an overall downhill two-step reaction with a stable intermediate. Thus, in the general reaction scheme

$$A \rightleftharpoons B \xrightarrow{k_2} C \qquad (17)$$

the first step is in "pre-equilibrium" with free-energy change $\Delta G_1 < 0$. The second step has a rate constant $k_2 = A_2 \exp(-E_2/RT)$ with $E_2 < -\Delta G_1$. The overall rate constant is

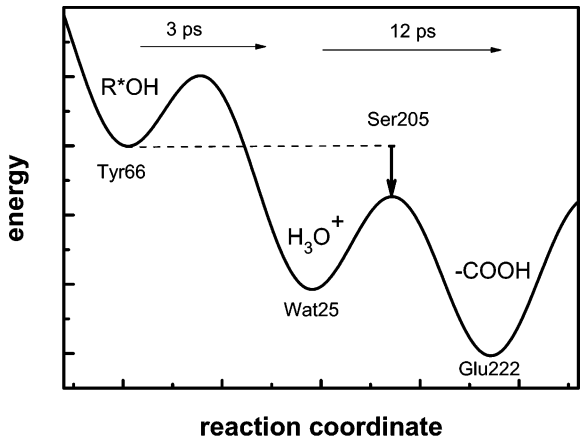

Figure 8. Qualitative two-step energy profile for proton dissociation from GFP that can lead to an overall negative activation energy (vertical arrow). The first downhill step from Tyr66 to Wat25 is larger than the second uphill step leading to the Ser205 intermediate. The heights of the two barriers correspond to the relative magnitudes of the two measured time constants,[5] depicted above the horizontal arrows.

then $k_d = A_2 \exp(-E_A/RT)$, with $E_A = E_2 + \Delta G_1 < 0$. This situation is portrayed schematically in Figure 8, with the negative activation energy depicted by the downward vertical arrow.

In GFP, room-temperature measurements with faster time resolution indeed exhibit two time constants for the dissociation stage (3 and 12 ps).[5] It is thus tempting to identify the intermediate B in the above scheme as a H_3O^+ moiety which is "sandwiched" between the R^*O^- and Ser205 (Figure 8). From a more detailed investigation of the temperature dependence of the two fast exponents, one may be able to deduce the heights of the two barriers surrounding the hydronium intermediate. This is not possible to obtain from the current data due to the limited time-resolution of the TCSPC method.

An analogous two-step acid dissociation mechanism in solution ($ROH + H_2O \rightleftharpoons RO^-...H_3O^+ \rightarrow RO^- + H_3O^+$) was suggested by Eigen,[35] identified in theoretical calculations of acid dissociation in water,[36] and observed in ultrafast pump−probe spectra of photoacids.[37] Interestingly, the H_3O^+ intermedi-

ate was recently identified in time-resolved IR from acid−base pairs separated by a single water molecule.[38] The present work obtains the stabilization energy of such an intermediate within GFP.

The above interpretation is at odds with a recent suggestion[13] that the first proton translocation along the wire is between Ser205 and Glu222 (rather than from Tyr66 to Wat25; see Figure 1). This suggestion is based upon unrelaxed gas-phase calculations in which the barrier for an initial Ser205 → Glu222 step is smaller than that for Tyr66 → Wat25. Yet, this barrier exceeds 42 kJ/mol, requiring the cleavage of a covalent O−H bond, which is not likely to occur on a 10 ps time scale.

The stabilization of the H_3O^+ intermediate likely requires some conformational changes in the surrounding protein residues, which optimize the HB around it (see discussion of Figure 5A in ref 15). Possibly, such motions are impeded below 220 K, when k_d shows normal temperature dependence (decreasing with decreasing T). This suggests that the extra stabilization of the hydronium, which resulted in the negative activation energy above 230 K, can no longer occur on the 10 ps time scale.

4.2. Glutamate 222 Protonation. It is conventionally assumed[8,9] that in the ground state Glu222 is anionic (i.e., dissociated), that it gets protonated in the ES by the proton which dissociates from Tyr66, and is thus the final stop for the photodissociated proton during the ES lifetime (ca. 3 ns) of the GFP chromophore. The ES protonation of Glu222 is corroborated by the increase (following the laser flash) in the time-resolved IR signal at 1711 cm^{-1}, assigned to a COOD mode of Glu222 in D_2O.[10−12] Time-resolved measurements of R*OH fluorescence over a short time scale (a fraction of a nanosecond)[5] exhibit fast biexponential decay which is expected from such a scenario. Yet, monitoring over a longer time scale reveals the power-law tail in the R*OH fluorescence,[17−19] which is inconsistent with the conventional interpretation.

Implicit in all the treatments to-date is the assumption that there is only one proton within GFP that may participate in the dynamics: the proton which dissociates from the hydroxyl moiety of the excited Tyr66. But, if Glu222 is anionic, where is its counterproton? Perhaps it is within the GFP? Since the relevant simulations for GFP have not yet been performed, one might obtain some insight from recent simulations for the D-pathway in cytochrome *c* oxidase.[39] These simulations show that a proton is stabilized on an internal water cluster not far from the anionic Glu286 (which is close to the active site), and it may be the primary source for reprotonation of this glutamate residue.

A similar situation may prevail in wt-GFP. As Figure 9 shows, there is a cluster of three water molecules on the other side of Glu222. A proton may be trapped on this cluster, forming an ion pair with the anion of Glu222. The photoexcited chromophore may modulate the pK_a of Glu222 sufficiently for inducing reprotonation by this proton. The second proton, which dissociates from Tyr66, may then replace it by a concerted process of double proton transfer:

$$H^+ + O=\overset{|}{C}\,OH \rightleftharpoons HO\,\overset{|}{C}=O + H^+$$

This reversible reaction bridges the proton wires on the two sides of Glu222, allowing the proton to migrate and occasionally return to the chromophore.

4.3. Proton Migration. The $t^{-1/2}$ decay of the (lifetime-corrected) fluorescence signal below 220 K is typical of a 1D diffusion process and was shown to agree quantitatively with the solution of a diffusion equation for 1D geminate recombination.[19] This suggests that the proton migrates along a 1D proton-wire within the GFP. Since a proton-wire is observed in the X-ray structure to extend beyond Glu222 (Figure 1) it could be the likely origin for this 1D diffusion. Below 110 K, thermal motion becomes so restrictive as to preclude free proton hops along this pathway. Above 230 K, the same behavior holds up to intermediate times, when a switch to the steeper $t^{-3/2}$ power law occurs.

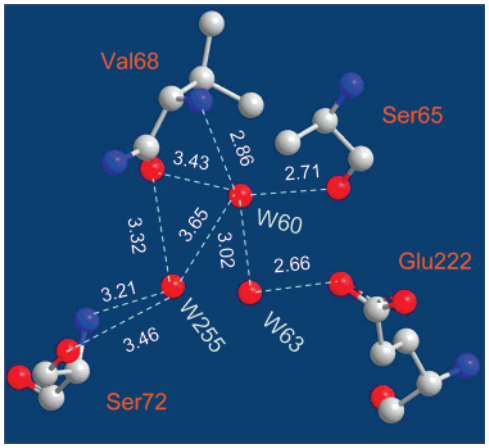

Figure 9. Cluster of three water molecules near Glu222 in wt-GFP which may promote its dissociation but retain the dissociated proton. This figure was prepared from PDB file 1GFL[7] (the A subunit) using Chem3D version 9: (red) oxygen, (blue) nitrogen, (gray) carbon. Hydrogens are not resolved in the X-ray structure, so that only water (W) oxygens are visible.

We can estimate a minimal value for the diffusive barrier, E_D, from the following argument. The last hop, Wat25 → Tyr66, involves a barrier of $E_D/2$. This follows from our observation that k_a^2/D is constant. On the other hand, it must be larger than the negative activation energy for dissociation, 5.6 kJ/mol (see Figure 8). Thus $E_D > 11.2$ kJ/mol, which is approximately the barrier height for proton mobility in liquid water.[40] Thus, although we cannot determine the value of the diffusion constant within the protein, at least we can show that it is slower than proton diffusion in water.

It is not self-evident that a proton can move diffusively within a protein. At least, there should not be very high barriers or deep wells along the pathway that could trap the proton and impede its migration. Free energy profiles along proton-wires within GFP have not yet been calculated. As noted in the Introduction, algorithms for achieving this goal are now available.[21,22] One may thus anticipate that the relevant calculations would be performed in the near future.

4.4. Switch Kinetics. The present work completes the picture of proton migration within wt-GFP for $T > 230$ K. It appears that after proton dissociation, Thr203 rotates (time constant τ) and forms an HB with the hydroxide of Tyr66, as previously suggested.[8] The added complication to this scenario is that this HB may allow proton exit (Figure 4). Whenever the proton, which is meanwhile migrating along the 1D wire of Figure 1, returns to Wat25, a process of proton escape is initiated. Possibly, there is concerted transfer here: the proton on Thr203 hops out while that from Hydronium25 replaces it (rate constant k_q). As a result, the power-law asymptotics changes from $t^{-1/2}$ to $t^{-3/2}$. The quantitative solution of the kinetics of eq 11 indeed fits the experimental data with only three parameters that need to be adjusted at each temperature. In contrast, when the exit path emanates from a point even slightly displaced from the origin of the wire (at Wat25), the decay no longer possesses the correct experimental shape, as demonstrated by Figure 7. This is corroborated by the X-ray structure (Figure 1), which

exhibits a second short pathway emanating from Tyr66 and leading (for a rotated Thr203) to the protein surface.[15] It is interesting that the two-pathway scenario is common with other proteins of the GFP family.[16]

While the change in the asymptotic power law can be derived from the earlier work of Kim et al.[23] (see section 2), it is instructive to understand on a more pedestrian level how this comes about. The hydroxyl on Tyr66 of the excited chromophore serves to donate its proton, on an ultrafast time scale, to the adjacent water molecule considered here as the origin of the proton-wire ($x = 0$). Thereafter, it behaves as a spectator which, due to its fast de-/reprotonation rate constants (k_d and k_a), simply monitors the proton probability to return to the origin of its random walk, $p(0,t|0)$. On a long time scale, the probability of observing a bound proton is very low so that the chromophore is only a small perturbation to the wire dynamics. It remains therefore to consider eq 2 with $k_d = 0$, $k_a = 0$, and $x_0 = 0$, depicting 1D diffusion on a semi-infinite line of a proton initially placed on its closed end. This is a classical problem in irreversible geminate recombination,[41] only restricted here to 1D.

When $k_q = 0$, no reaction occurs and the complete solution consists of two Gaussians depicting reflection in the boundary at $x = 0$. The probability of return to the origin is then

$$p_0(0,t|0) = (\pi D t)^{-1/2} \tag{18a}$$

When $k_q > 0$, the solution becomes (e.g., eq 3.11a in ref 23) the following:

$$p(0,t|0) = p_0(0,t|0) - \frac{k_q}{D}\Omega(k_q\sqrt{t/D}) \sim \frac{1}{{k_q}^2}\sqrt{\frac{D}{4\pi t^3}} \tag{18b}$$

Here $\Omega(z)$ is defined by eq 7. By inserting its asymptotic expansion[28] into eq 7, one finds that the first-order term cancels identically, leaving the second-order term with its $t^{-3/2}$ dependence. Note also that $P(t)$ of eq 9a is related to $p(0,t|0)$ by detailed balancing: $k_d P(t) = k_a p(0,t|0)$. One concludes that the switchover in the asymptotics occurs already when an irreversible sink is activated at the origin of a 1D diffusion problem. It is thus an inherent property of a proton-wire with an escape route, independent of the added reversible binding site.

The temperature dependence of the ultimate $t^{-3/2}$ phase is mainly contributed by the activation barrier for the switch opening. The latter is governed by the rotation of the Thr203 side chain for which we find an activation enthalpy of 27 kJ/mol. Side-chain rotations within a protein are rarely determined experimentally. One exception involves side-chain relaxation within the myoglobin heme pocket (Table 10 in ref 42). For leucine, possessing a side chain of similar size to that of threonine, the activation enthalpy was found to be 21−23 kJ/mol. The present value is just slightly higher, which might be attributed to a weak HB formed by the hydroxyl moiety of Thr203 in its "open" state (as opposed to the methyl group of Leu which cannot form such a bond). This then adds to the pure rotational barrier for side-chain isomerization.

5. Conclusion

The close agreement demonstrated herein between time-resolved measurements on GFP and a 1D diffusion model for a switchable proton-wire argues in favor of this model. The emerging picture is that the dissociated proton (10 ps) initially migrates along an internal proton-wire which extends within the protein beyond Glu222. After some time (ca. 300 ps at room temperature), Thr203 rotates and forms an HB to the anionic chromophore. This allows an irreversible proton escape to the external protein surface, which is manifested in a change of the asymptotic behavior from $t^{-1/2}$ to $t^{-3/2}$.

Further experiments, such as point mutations, may shed additional light on this mechanism. One may expect that eliminating the switch (e.g., by a Thr203Leu mutation) would eliminate the $t^{-3/2}$ phase in the asymptotic kinetics by disallowing proton escape. Disconnecting the proton-wire from the chromophore (e.g., a Ser205Ala mutation) should eliminate the low-T power law but still allow proton escape. The dual mutation is subsequently expected to prevent proton dissociation altogether, rendering the GFP fluorescence blue (R*OH) rather than green (R^*O^-). Such mutation work should nevertheless be accompanied by X-ray structure determination, since proton pathways depend sensitively on small changes in their vicinity and mutations sometimes lead to unpredictable changes. Thus, elucidation of the microscopic mechanism behind GFP fluorescence may contribute toward planned strategies for bioengineering of GFP mutants.

Acknowledgment. I thank Ai Shinobu for preparing the graphics for Figure 1 and Soohyung Park for comments on the manuscript. This research was supported in part by The Israel Science Foundation (Grant No. 191/03).

References and Notes

(1) Wraight, C. A. *Biochim. Biophys. Acta* **2006**, *1757*, 886−912.
(2) Frank, R. A. W.; Titman, C. M.; Pratap, J. V.; Luisi, B. F.; Perham, R. N. *Science* **2004**, *306*, 872−876.
(3) Zimmer, M. *Chem. Rev.* **2002**, *102*, 759−781.
(4) Agmon, N. *J. Phys. Chem. A* **2005**, *109*, 13−35.
(5) Chattoraj, M.; King, B. A.; Bublitz, G. U.; Boxer, S. G. *Proc. Nat. Acad. Sci. U.S.A.* **1996**, *93*, 8362−8367.
(6) Lossau, H.; Kummer, A.; Heinecke, R.; Pöllinger-Dammer, F.; Kompa, C.; Bieser, G.; Jonsson, T.; Silva, C. M.; Yang, M. M.; Youvan, D. C.; Michel-Beyerle, M. E. *Chem. Phys.* **1996**, *213*, 1−16.
(7) Yang, F.; Moss, L. G.; Phillips, G. N., Jr. *Nature Biotech.* **1996**, *14*, 1246−1251.
(8) Brejc, K.; Sixma, T. K.; Kitts, P. A.; Kain, S. R.; Tsien, R. Y.; Ormö, M.; Remington, S. J. *Proc. Nat. Acad. Sci. U.S.A.* **1997**, *94*, 2306−2311.
(9) Palm, G. J.; Zdanov, A.; Gaitanaris, G. A.; Stauber, R.; Pavlakis, G. N.; Wlodawer, A. *Nature Struct. Biol.* **1997**, *4*, 361−365.
(10) van Thor, J. J.; Zanetti, G.; Ronayne, K. L.; Towrie, M. *J. Phys. Chem. B* **2005**, *109*, 16099−16108.
(11) Stoner-Ma, D.; Jaye, A. A.; Matousek, P.; Towrie, M.; Meech, S. R.; Tonge, P. J. *J. Am. Chem. Soc.* **2005**, *127*, 2864−2865.
(12) Stoner-Ma, D.; Melief, E. H.; Nappa, J.; Ronayne, K. L.; Tonge, P. J.; Meech, S. R. *J. Phys. Chem. B* **2006**, *110*, 22009−22018.
(13) Vendrell, O.; Gelabert, R.; Moreno, M.; Lluch, J. M. *J. Am. Chem. Soc.* **2006**, *128*, 3564−3574. This work does not include dynamic effects. The description is quite different when dynamics is considered (Gelabert, R. Personal communication).
(14) Wang, S.; Smith, S. C. *Phys. Chem. Chem. Phys.* **2007**, *9*, 452−458.
(15) Agmon, N. *Biophys. J.* **2005**, *88*, 2452−2461.
(16) Schäfer, L. V.; Groenhof, G.; Klingen, A. R.; Ullmann, G. M.; Boggio-Pasquaand, M.; Robb, M. A.; Grubmüller, H. *Angew. Chem., Int. Ed.* **2007**, *46*, 530−536.
(17) Leiderman, P.; Ben-Ziv, M.; Genosar, L.; Huppert, D.; Solntsev, K. M.; Tolbert, L. M. *J. Phys. Chem. B* **2004**, *108*, 8043−8053.
(18) Huppert, D.; Leiderman, P.; Ben-Ziv, M.; Genosar, L.; Cohen, L. *J. Phys. Chem. B* **2005**, *109*, 4241−4251.
(19) Leiderman, P.; Huppert, D.; Agmon, N. *Biophys. J.* **2006**, *90*, 1009−1018.
(20) Agmon, N.; Pines, E.; Huppert, D. *J. Chem. Phys.* **1988**, *88*, 5631−5638.
(21) Olsson, M. H. M.; Sharma, P. K.; Warshel, A. *FEBS Lett.* **2005**, *579*, 2026−2034.
(22) Voth, G. A. *Acc. Chem. Res.* **2006**, *39*, 143−150.
(23) Kim, H.; Shin, K. J.; Agmon, N. *J. Chem. Phys.* **1999**, *111*, 3791−3799.
(24) Gopich, I. V.; Solntsev, K. M.; Agmon, N. *J. Chem. Phys.* **1999**, *110*, 2164−2174.

(25) Kim, H.; Shin, K. J.; Agmon, N. *J. Chem. Phys.* **2001**, *114*, 3905−3912.
(26) Kim, H.; Shin, K. J. *J. Chem. Phys.* **2004**, *120*, 9142−9150.
(27) Krissinel', E. B.; Agmon, N. *J. Comput. Chem.* **1996**, *17*, 1085−1098.
(28) Abramowitz, M., Stegun, I. A., Eds.; *Handbook of Mathematical Functions*; Dover: New York, 1970.
(29) Agmon, N. *J. Chem. Phys.* **1984**, *81*, 2811−2817.
(30) Agmon, N. *Chem. Phys. Lett.* **2006**, *417*, 530−534.
(31) Winkler, K.; Lindner, J.; Bürsing, H.; Vöhringer, P. *J. Chem. Phys.* **2002**, *113*, 4674−4682.
(32) Leiderman, P.; Gepshtein, R.; Uritski, A.; Genosar, L.; Huppert, D. *J. Phys. Chem. A* **2006**, *110*, 9039−9050.
(33) Singleton, D. L.; Cvetanović, R. J. *J. Am. Chem. Soc.* **1976**, *98*, 6812−6819.
(34) Mozurkewich, M.; Benson, S. W. *J. Phys. Chem.* **1984**, *88*, 6429−6435.
(35) Eigen, M. *Angew. Chem., Int. Ed.* **1964**, *3*, 1−72.
(36) Ando, K.; Hynes, J. T. *J. Phys. Chem. B* **1997**, *101*, 10464−10478.
(37) Leiderman, P.; Genosar, L.; Huppert, D. *J. Phys. Chem. A* **2005**, *109*, 5965−5977.
(38) Mohammed, O. F.; Pines, D.; Dreyer, J.; Pines, E.; Nibbering, E. T. J. *Science* **2005**, *310*, 83−86.
(39) Xu, J.; Sharpe, M. A.; Qin, L.; Ferguson-Miller, S.; Voth, G. A. *J. Am. Chem. Soc.* **2007**, *129*, 2910−2913.
(40) Agmon, N. *J. Chim. Phys. Phys.*−*Chim. Biol.* **1996**, *93*, 1714−1736.
(41) Rice, S. A. *Diffusion-Limited Reactions*; Comprehensive Chemical Kinetics; Elsevier: Amsterdam, 1985; Vol. 25.
(42) Dantsker, D.; Samuni, U.; Friedman, J. M.; Agmon, N. *Biochim. Biophys. Acta: Proteins Proteomics* **2005**, *1749*, 234−251.